Report

Current Biology

Natural *C. elegans* Microbiota Protects against Infection via Production of a Cyclic Lipopeptide of the Viscosin Group

Graphical Abstract

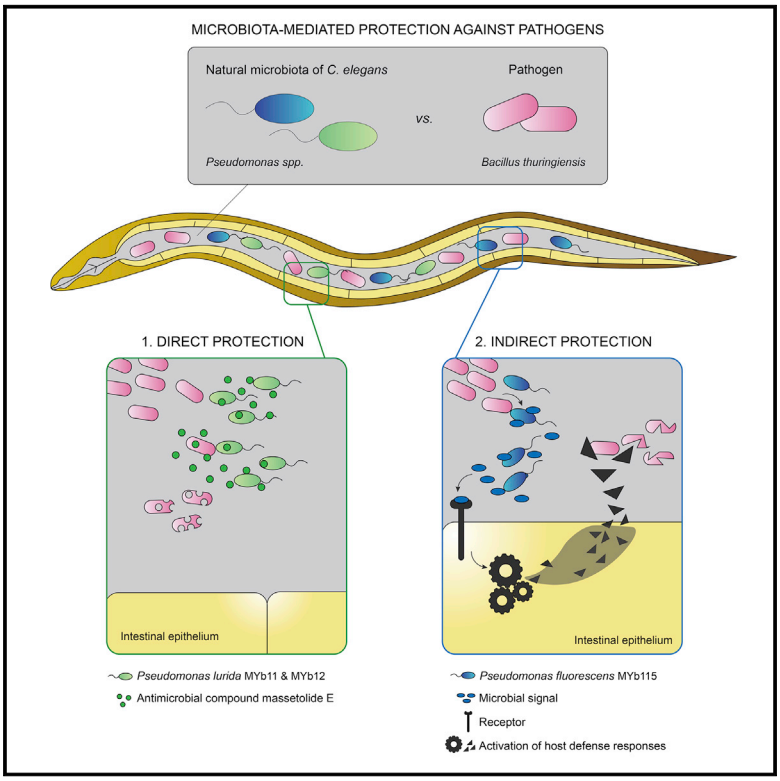

Highlights

- Natural *C. elegans* microbiota confer protection against pathogen infection
- Different *Pseudomonas* isolates protect *C. elegans* through distinct mechanisms
- *P. lurida* isolates produce massetolide E and directly inhibit pathogen growth
- *P. fluorescens*-mediated protection may depend on indirect, host-mediated mechanisms

Authors

Kohar A.B. Kissoyan, Moritz Drechsler, Eva-Lena Stange, Johannes Zimmermann, Christoph Kaleta, Helge B. Bode, Katja Dierking

Correspondence

kdierking@zoologie.uni-kiel.de

In Brief

Kissoyan et al. provide novel insights into the function of the native microbiota of the model nematode *C. elegans*. Their work highlights the role of microbes in supporting *C. elegans* defense responses and the diversity of immune-protective mechanisms, including the involvement of microbiota-derived metabolites.

Kissoyan et al., 2019, Current Biology *29*, 1–8
March 18, 2019
https://doi.org/10.1016/j.cub.2019.01.050

CellPress

Please cite this article in press as: Kissoyan et al., Natural *C. elegans* Microbiota Protects against Infection via Production of a Cyclic Lipopeptide of the Viscosin Group, Current Biology (2019), https://doi.org/10.1016/j.cub.2019.01.050

Current Biology
Report

Natural *C. elegans* Microbiota Protects against Infection via Production of a Cyclic Lipopeptide of the Viscosin Group

Kohar A.B. Kissoyan,[1] Moritz Drechsler,[2] Eva-Lena Stange,[1] Johannes Zimmermann,[4] Christoph Kaleta,[4] Helge B. Bode,[2,3] and Katja Dierking[1,5,*]

[1]Department of Evolutionary Ecology and Genetics, Zoological Institute, Christian-Albrechts-Universität zu Kiel, 24118 Kiel, Germany
[2]Fachbereich Biowissenschaften, Goethe Universität Frankfurt, 60438 Frankfurt am Main, Germany
[3]Buchmann Institute for Molecular Life Sciences, Goethe Universität Frankfurt, 60438 Frankfurt am Main, Germany
[4]Research Group Medical Systems Biology, Institute of Experimental Medicine, Christian-Albrechts-Universität zu Kiel, 24105 Kiel, Germany
[5]Lead Contact
*Correspondence: kdierking@zoologie.uni-kiel.de
https://doi.org/10.1016/j.cub.2019.01.050

SUMMARY

Caenorhabditis elegans is associated in nature with a species-rich, distinct microbiota, which was characterized only recently [1]. Thus, our understanding of the relevance of the microbiota for nematode fitness is still at its infancy. One major benefit that the intestinal microbiota can provide to its host is protection against pathogen infection [2]. However, the specific strains conferring the protection and the underlying mechanisms of microbiota-mediated protection are often unclear [3]. Here, we identify natural *C. elegans* microbiota isolates that increase *C. elegans* resistance to pathogen infection. We show that isolates of the *Pseudomonas fluorescens* subgroup provide paramount protection from infection with the natural pathogen *Bacillus thuringiensis* through distinct mechanisms. We found that the *P. lurida* isolates MYb11 and MYb12 (members of the *P. fluorescens* subgroup) protect *C. elegans* against *B. thuringiensis* infection by directly inhibiting growth of the pathogen both *in vitro* and *in vivo*. Using genomic and biochemical analyses, we further demonstrate that MYb11 and MYb12 produce massetolide E, a cyclic lipopeptide biosurfactant of the viscosin group [4, 5], which is active against pathogenic *B. thuringiensis*. In contrast to MYb11 and MYb12, *P. fluorescens* MYb115-mediated protection involves increased resistance without inhibition of pathogen growth and most likely depends on indirect, host-mediated mechanisms. This work provides new insight into the functional significance of the *C. elegans* natural microbiota and expands our knowledge of bacteria-derived compounds that can influence pathogen colonization in the intestine of an animal.

RESULTS AND DISCUSSION

Surprisingly little is known about the ecology of the model nematode *Caenorhabditis elegans*. The natural microbiota of *C. elegans* was characterized only recently [1] and its effects on worm fitness remain to be uncovered. Here, we systematically tested which members of the *C. elegans* microbiota protect the worm from infection with its natural pathogen, *Bacillus thuringiensis*. We selected 13 isolates that comprise the most abundant genera of the *C. elegans* natural core microbiome, namely *Pseudomonas*, *Ochrobactrum*, and *Acinetobacter* [6], and that are able to enter and persist in the nematode gut [1]. First, we assessed population growth (as proxy for fitness) of the natural *C. elegans* isolate MY316, which was co-isolated with the microbiota isolates, 5 days after exposure to the nematicidal *B. thuringiensis* strains MYBT18247(BT247) mixed with the respective microbiota isolate or with the laboratory food bacterium *Escherichia coli* OP50 as control. The non-nematicidal *B. thuringiensis* strain BT407 served as non-pathogen control. We found that worms on pathogenic BT247 showed a clear increase in population growth when infected in the presence of five microbiota isolates—all of the genus *Pseudomonas*—compared to infected worms on *E. coli* OP50 (Figure 1A). Moreover, worms on the non-pathogenic BT407 also showed increased population growth in the presence of the *Pseudomonas* isolates (Figure S1A), indicating that these microbiota isolates also represent good growth environments for *C. elegans* under control conditions, confirming previous work [1]. We thus focused on the *Pseudomonas* microbiota isolates, which can be assigned to the following species based on complete 16S rRNA sequences: *P. lurida* MYb11, *P. lurida* MYb12, *P. fluorescens* MYb115, and *P. lurida* MYb193 (all of the *P. fluorescens* group), *P. denitrificans* MYb185 (*P. pertucinogena* group), and *P. alkylphenolia* MYb187 (*P. putida* group). We then asked if they also affect the fitness of the *C. elegans* reference laboratory strain N2. Indeed, BT247 infected N2 worms showed increased population growth in the presence of all six *Pseudomonas* isolates (MYb11, MYb12, MYb115, MYb185, MYb187, and MYb193), albeit statistically significant only for MYb115 (Figure 1B). N2 worms on the

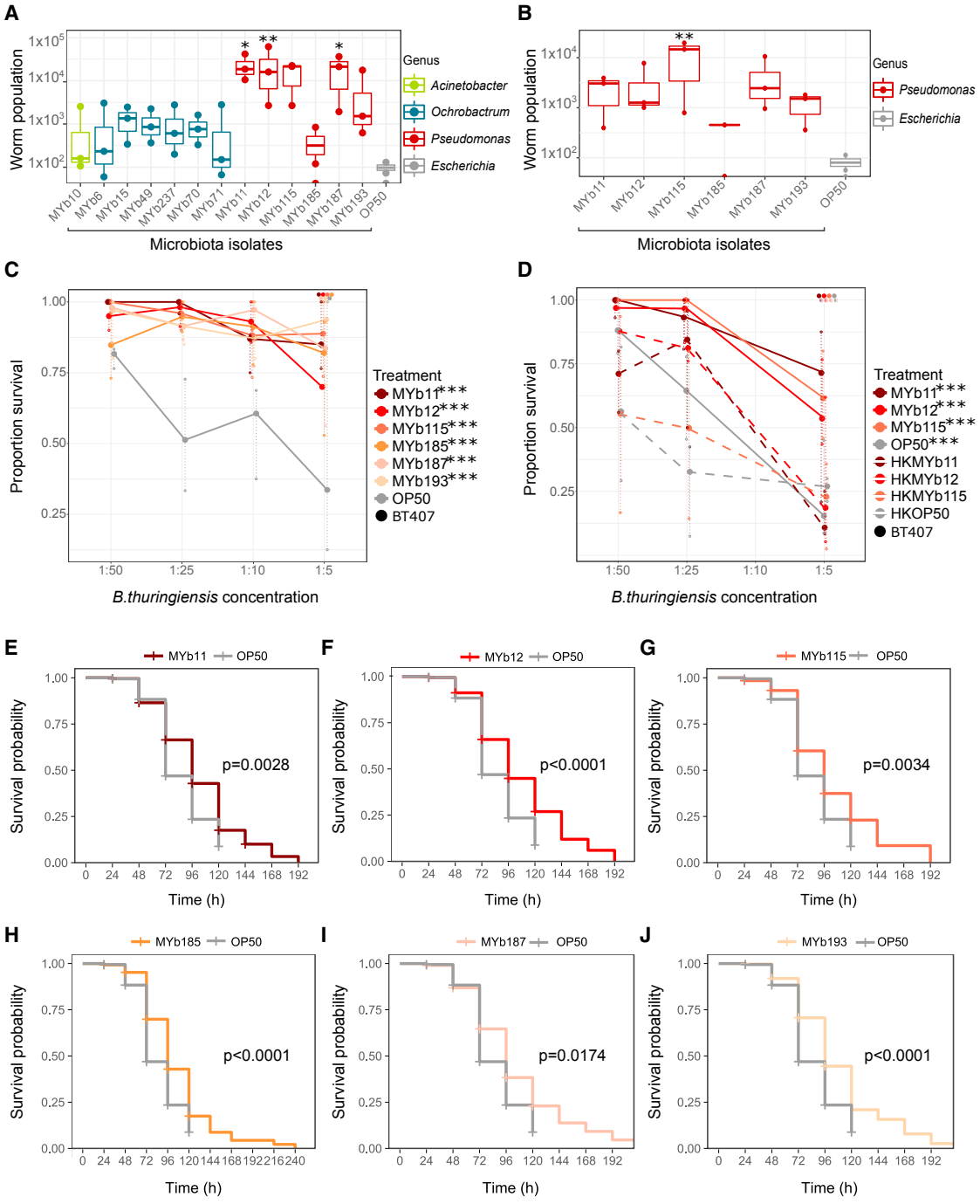

Figure 1. Natural Microbiota Isolates of the Genus *Pseudomonas* Protect *C. elegans* from Pathogen Infection

(A and B) Population size measured in the presence of pathogenic *B. thuringiensis* BT247 of (A) the natural *C. elegans* isolate MY316 on one of 13 microbiota isolates and (B) the laboratory N2 reference strain on one of six *Pseudomonas* isolates. The food bacterium *E. coli* OP50 was used as control. Three L4 larvae were picked onto the infection plates. Population size was assessed after 5 days at 20°C. The boxplots indicate the median, range, and upper and lower quartiles of the worm population data (n = 3 independent runs). Statistical analysis was performed using generalized linear model (GLM) [7] framework and the obtained p values were corrected using Bonferroni correction for multiple testing [8].

(C and D) Survival of *C. elegans* N2 on different concentrations of pathogenic BT247 mixed with either (C) one of six living *Pseudomonas* isolates or (D) one of the three *Pseudomonas* isolates—MYb11, MYb12, and MYb115—alive (continuous lines) or heat killed (dashed lines). *E. coli* OP50 was used as control and the *B. thuringiensis* strain BT407 as non-pathogen control. Error bars represent the range of the median of survival proportions of four technical replicates (n = 4), representative of at least three independent runs. Statistical analyses were performed using GLM [7] framework and Bonferroni correction for multiple testing [8] with the OP50 control treatment group.

(legend continued on next page)

non-pathogenic BT407 also showed increased median population growth in the presence of four *Pseudomonas* isolates (Figure S1B). This might point to differences in nutritional qualities between the different *Pseudomonas* isolates, which was previously suggested to underlie the ability of different bacteria to affect *C. elegans* physiological processes such as development, growth, aging, and longevity [11].

We considered that increased resistance to BT infection may contribute to the observed increased fitness of infected worms on natural microbiota isolates. We thus challenged *C. elegans* N2 worms on the respective *Pseudomonas* isolates with pathogenic BT247 at different concentrations and assessed survival 24 h post infection (p.i.) as proxy for resistance. We found that worms on all tested *Pseudomonas* isolates showed significantly increased survival when compared to infected worms on *E. coli* OP50 (Figure 1C). Taken together, these results show that *C. elegans* microbiota isolates of the genus *Pseudomonas* provide paramount protection from infection with *B. thuringiensis* MYBT247. In previous work, the *Pseudomonas* isolates MYb11, MYb187, and MYb193 have been reported to inhibit fungal growth *in vitro* [1]. Importantly, MYb11 protected the nematode from infection by the fungal pathogen *Drechmeria coniospora* also *in vivo* through a hitherto unknown mechanism [1]. Our work thus extends our knowledge on the protective effect of MYb11 to bacterial infection in the intestine.

It was previously shown that *P. mendocina*, which is a member of laboratory-established *C. elegans* microbiota, protects the worm against infection with pathogenic *P. aeruginosa* PA14 [12]. While *P. aeruginosa* PA14 is not a natural *C. elegans* pathogen, it is one of the most extensively studied *C. elegans* pathogens [13, 14]. To investigate if the protection conferred by the *Pseudomonas* isolates is specific against infection with the Gram-positive pathogen *B. thuringiensis* or rather is a generic protection against a broader range of pathogens, we assessed survival of worms grown on the respective microbiota isolates or on *E. coli* OP50 from the L1 stage and infected with the Gram-negative *P. aeruginosa* PA14 at the L4 stage. We observed prolonged survival for worms on all six *Pseudomonas* isolates tested (Figures 1E–1J). This indicates that the *Pseudomonas* microbiota isolates confer resistance to PA14 infection, in addition to BT247 infection.

MYb11, MYb12, MYb115, MYb185, MYb187, and MYb193 confer resistance to Gram-positive, as well as Gram-negative, bacterial pathogens. This broader protective effect might be based on activation of general *C. elegans* defense responses. The aforementioned *P. mendocina* protects *C. elegans* against infection with PA14 likely through activation of p38 MAPK signaling [12], an innate immune signaling pathway central for *C. elegans* defense against several different pathogens [13]. However, apart from this one example, the mechanisms by which the *C. elegans* microbiota protects the worm from pathogen infection are completely unknown. Intestinal microbiota can confer protection against intestinal pathogens in two ways: through indirect activation of the host immune response or through direct microbe-microbe competition [3, 15, 16]. In a first step toward exploring the molecular mechanism underlying the observed microbiota-mediated protection, we tested whether the protective effects require alive bacteria and assessed worm survival after BT247 infection in the presence of both alive and heat-inactivated microbiota isolates MYb11, MYb12, and MYb115, which strongly and consistently protected *C. elegans* from *B. thuringiensis* infection. Worms on heat-inactivated MYb11, MYb12, and MYb115 showed significantly decreased survival compared to worms on alive microbiota isolates (Figure 1D), indicating that bacterial metabolic activity is required for the protective effect.

We then asked whether the protective effect is provided through direct microbe-microbe antagonism—i.e., if the *Pseudomonas* isolates directly inhibit pathogen growth. To answer this question, we first tested the effect of cell-free supernatant of the six *Pseudomonas* isolates (MYb11, MYb12, MYb115, MYb185, MYb187, and MYb193) on pathogen growth in a disc-diffusion assay *in vitro*. While the supernatant of MYb11 and MYb12 strongly inhibited growth of *B. thuringiensis* BT247, supernatant of the other protective *Pseudomonas* isolates did not have an effect on *B. thuringiensis* growth (Figure 2A). In contrast, none of the *Pseudomonas* isolates inhibited growth of *P. aeruginosa* PA14 (Figure 2B). We are currently investigating how *Pseudomonas* microbiota isolates protect the worm from PA14 infection. Here, we focused on MYb11 and MYb12, the only *Pseudomonas* isolates showing antagonistic properties against BT247. When we investigated the range of antagonistic activity of MYb11 and MYb12 supernatant on several Gram-positive and Gram-negative bacteria, we found that growth of all tested *B. thuringiensis* strains and growth of *Staphylococcus aureus* SA113 was strongly inhibited (Figures S2A–S2D). In contrast, MYb11 and MYb12 supernatant did not inhibit growth of the Gram-positive natural isolates *Leucobacter tardus* MYb258 and *Rhodococcus erythropolis* MYb53 or any of the tested Gram-negative bacteria (Figures S2A–S2D). Taken together, our results suggest that the two *P. lurida* isolates MYb11 and MYb12 have antagonistic capacities and directly inhibit the growth of *B. thuringiensis* through the production of bacteriostatic and/or bactericidal compounds. In contrast, the other *Pseudomonas* isolates might protect the nematode from BT247 infection through distinct mechanisms.

To further explore the potentially distinct mechanisms underlying the observed microbiota-mediated protection from BT247 infection, we subsequently focused on the microbiota isolates MYb11, MYb12, and MYb115. All three consistently protected *C. elegans* from BT247 infection, while only MYb11 and MYb12 inhibited *B. thuringiensis* growth *in vitro*. Next, we investigated if MYb11, MYb12, and MYb115 inhibit growth of *B. thuringiensis in vivo* and thus infected *C. elegans* with BT247 mixed with MYb11, MYb12, MYb115, or *E. coli* OP50. We assessed pathogen load 24 h p.i. by counting colony-forming

(E–J) Survival of *C. elegans* N2 on pathogenic *P. aeruginosa* PA14 grown on any of the six *Pseudomonas* isolates, (E) MYb11, (F) MYb12, (G) MYb115, (H) MYb185, (I) MYb187, and (J) MYb193. Kaplan-Meier analysis was followed by log-rank test [9] and Bonferroni correction [10]. The graphs are based on pooled data of three independent runs, each with four technical replicates with at least 30 worms per plate and treatment condition. Worms were grown from L1 stage on the subsequent microbiota isolate and infected at the L4 stage on slow-killing PA14 plates. Alive worms were transformed daily to fresh PA14 infection plates. p values are considered significant and denoted with asterisks according to *$p < 0.05$, **$p < 0.01$, ***$p < 0.001$. See also Figure S1.

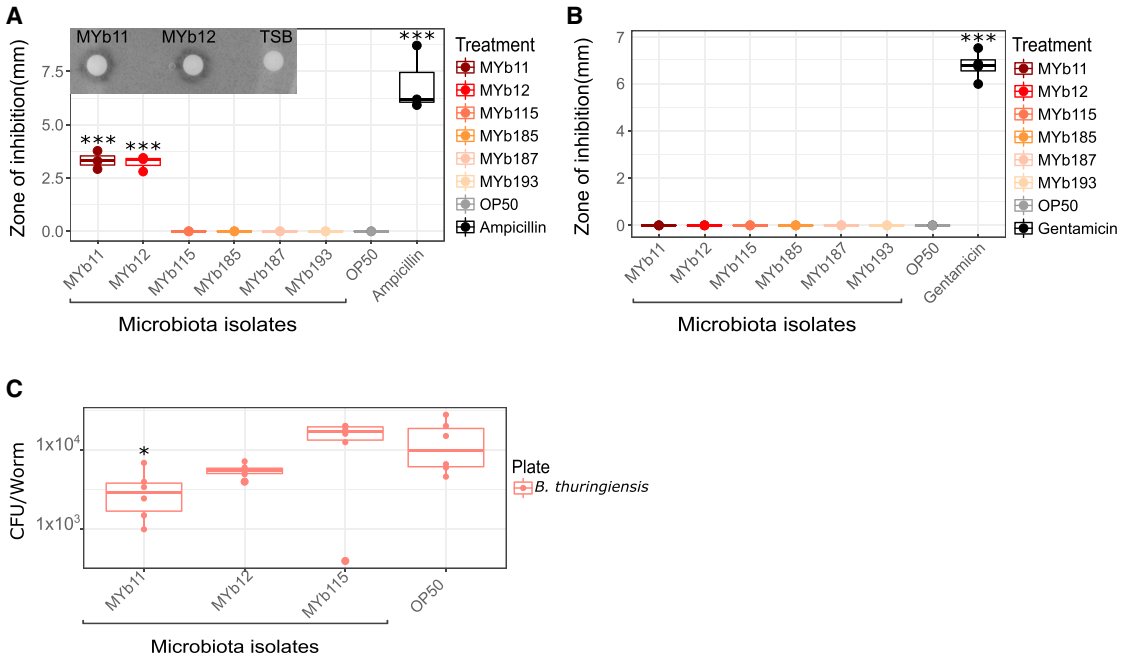

Figure 2. *Pseudomonas lurida* MYb11 and MYb12 Have Antagonistic Activity and Inhibit Pathogen Growth *In Vitro* and *In Vivo*

(A and B) Growth inhibition of (A) *B. thuringiensis* BT247 and (B) *P. aeruginosa* PA14 by cell-free supernatant of the six *Pseudomonas* microbiota isolates, *E. coli* OP50, or a respective antibiotic as positive control measured as diameter of inhibition zone (mm) in a disc diffusion assay. The data points represent the mean diameter of three technical replicates of three independent runs (n = 3). The boxplots indicate the median, range, and upper and lower quartiles of the data. The diameters are standardized by subtracting the 6 mm diameter of the disc from the overall diameter measured. The inlay in (A) is a representative image of the disc diffusion assay showing that supernatant of MYb11 and MYb12 inhibit growth of BT247 in contrast to the TSB medium control. Student's t test against the OP50 control, followed by Bonferroni correction, was performed [8].

(C) Colonization of *C. elegans* intestine by BT247 in the presence of the *Pseudomonas* isolates MYb11, MYb12, and MYb115 or the *E.coli* OP50 control. Pathogen load was measured in a CFU assay. L4 larvae were exposed to BT247 mixed with the respective microbiota isolate or *E. coli* OP50 for 24 h. The boxplots indicate the median, range, and upper and lower quartiles of five technical replicates (n = 5). These data are representative of at least three independent runs.

p values are considered significant and denoted with asterisks according to *p $\leq$ 0.05, **p $\leq$ 0.01, ***p $\leq$ 0.001. See also Figure S2.

units (CFUs). We observed that pathogen load was clearly decreased in infected worms on MYb11 and MYb12, but not in worms on MYb115, when compared to worms on *E. coli* OP50 (Figure 2C). These results suggest that MYb11 and MYb12 control pathogen load *in vivo*, while MYb115 protects the worm from pathogenic impact without directly reducing pathogen load.

Worms on the *Pseudomonas* isolates MYb11, MYb12, and MYb115 show clearly increased fitness and resistance to *B. thuringiensis* infection. While MYb11 and MYb12 seem to protect worms through directly inhibiting pathogen growth, worms on MYb115 are protected despite a high pathogen burden. Accordingly, MYb115 might provide protection by limiting pathogen-induced damage to the intestinal epithelium. We thus asked whether the damage caused by *B. thuringiensis* infection is reduced in worms on MYb115, as well as on MYb11 and MYb12. *B. thuringiensis* produces spores that are associated with pore-forming toxins called Cry toxins [17, 18]. The damage caused by these toxins can lead to loss of intestinal barrier function. To assess the severity of the damage caused by infection, we measured *C. elegans* intestinal barrier function using the "smurf" assay [19], in which worms are exposed to blue dye. As long as intestinal barrier function is intact, the blue dye is contained in the intestine of worms. If intestinal integrity is disrupted, the dye leaks into the body cavity. We observed that the blue dye was indeed contained in the intestine of uninfected worms (Figure 3A, 3C, 3E, and 3G), while it leaked into the body cavity in control worms infected with BT247, thus displaying the smurf phenotype (arrows in Figure 3H). Notably, *B. thuringiensis*-induced disruption of intestinal barrier function was significantly reduced in BT247 infected worms on the *Pseudomonas* isolates MYb11, MYb12, and MYb115 (Figure 3B, 3D, 3F, and 3I). Together, our results indicate that MYb11 and MYb12 protect the host through direct antagonism, while MYb115 helps the host to cope with the infection despite a high pathogen burden. We are currently investigating if the effect of MYb115 is mediated by an indirect mechanism—i.e., through reinforcement of intestinal barriers, increased damage repair, or activation of other defense responses. However, we cannot exclude that MYb115 has a direct effect on the Cry toxins released by the BT spores—e.g., by degradation of the toxins—as was previously shown for a protease secreted by the probiotic *B. clausii* that inhibits the toxic effects of *B. cereus* toxins in a cytotoxicity assay using mammalian cell lines [20].

To identify the putative bacteriostatic and/or bactericidal compounds produced by MYb11 and MYb12, we analyzed extracts from bacterial cultures using ultra-performance liquid chromatography (UPLC) coupled with high-resolution mass

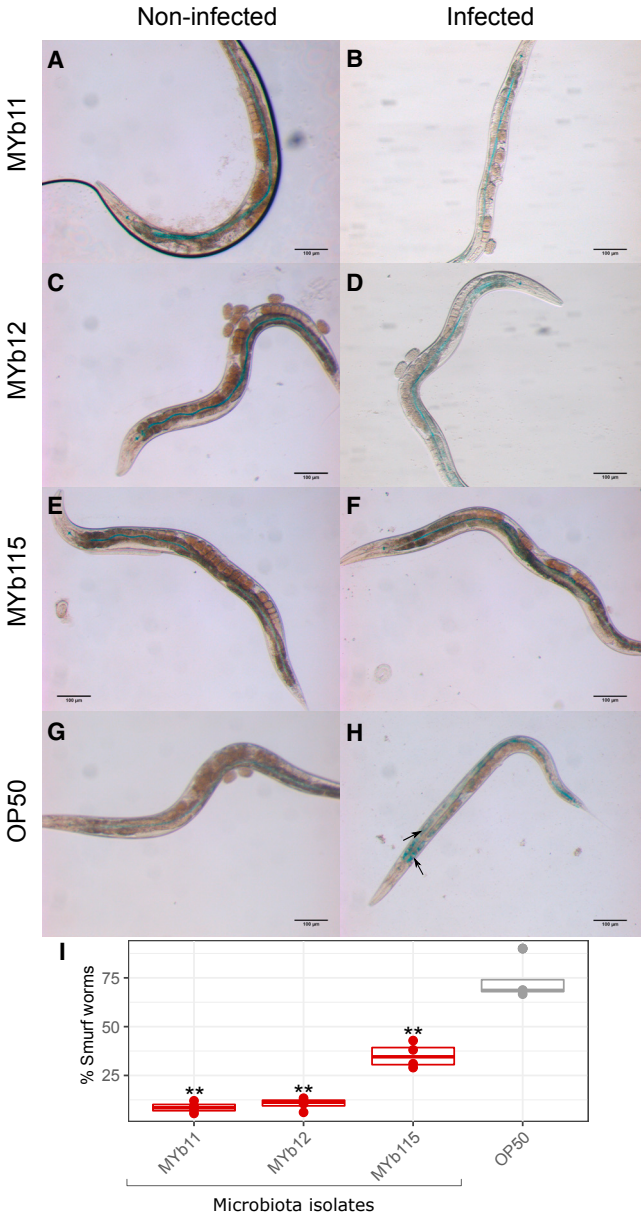

Figure 3. *B. thuringiensis*-Induced Disruption of Intestinal Barrier Integrity Is Reduced in Worms on *Pseudomonas* Isolates MYb11, MYb12, and MYb115

(A–H) Representative light-microscopy pictures of non-infected (panels on left side) and BT247-infected (panels on right side) worms on (A and B) MYb11, (C and D) MYb12, (E and F) MYb115, and (G and H) *E. coli* OP50. The blue dye is contained in the intestinal lumen of non-infected worms and worms on MYb11, MYb12, and MYb115 while it leaks into the body cavity of infected control worms (black arrows in H), showing the smurf phenotype.

(I) Quantification of the smurf phenotype. The percentage of smurf worms was calculated per treatment with at least 30 worms (n = 4 replicates). The boxplots indicate the median, range, and upper and lower quartiles of the data. Student's pairwise t test and Bonferroni-based adjustment were used to correct for multiple testing with the OP50 control treatment group [8]. These data are representative of two independent runs.

p values are considered significant and denoted with asterisks according to: $^{*}p \leq 0.05$, $^{**}p \leq 0.01$, $^{***}p \leq 0.001$.

spectrometry (HRMS). In parallel, we used antiSMASH to search for known biosynthetic gene clusters (BGCs) [21] in the genomes of MYb11 and MYb12. Both methods lead to the discovery of viscosin (*m/z* 1126.68 $[M+H]^+$; RT 12.1 min) and the viscosin BGC [22], respectively. To confirm that this compound is indeed active against the pathogens BT247 and BT679, we fractionated the extracts of MYb11 and MYb12 using preparative high-performance liquid chromatography (HPLC) and tested each fraction against both pathogens (Figure 4). We could show that the active compound against the two pathogens was not viscosin but instead massetolide E (*m/z* 1112.66 $[M+H^+]$; RT 11.9 min) (Figures 4 and S3). Massetolide E is a viscosin derivative that contains a valine residue instead of the Leu/Ile residue (Figure S4).

Massetolide E and viscosin are cyclic lipopeptide biosurfactants of the viscosin group synthesized by nonribosomal peptide synthetases (NRPSs) in *Pseudomonas* spp. isolated from soil- and plant-associated environments, as well as marine habitats [4, 5]. Massetolides and viscosin lipopeptides are known to have both antifungal and antibacterial activities, preferentially against Gram-positive bacteria [4, 5, 23, 24], which is in line with the protective effect of MYb11 and MYb12 against fungi [1] and the Gram-positive *B. thuringiensis* (this study). Interestingly, *B. subtilis*, which is not a member of the *C. elegans* natural microbiota but has been used to study host-microbe interactions in the worm, was reported to protect the worm from Gram-positive pathogens through fengycin-mediated microbial antagonism [25]. Fengycins are also cyclic lipopeptides that are produced by *Bacillus spp* [5] and were recently shown to inhibit *S. aureus* quorum sensing, which in turn was shown to be crucial for intestinal colonization by *S. aureus* in mice [26]. Interestingly, while the fengycin-mediated inhibitory effect was clearly linked to interference with quorum sensing, the *Bacillus* isolates investigated by Piewngam et al. only show a minor growth inhibitory effect on *S. aureus* [26]. This is in contrast to the strong growth inhibitory effect we observed for MYb11 and MYb12 supernatant on *S. aureus* (Figures S2A, S2B, and S2D) and might suggest that the mechanisms of bacterial growth inhibition between fengycin and massetolide E are distinct. These and our findings thus emphasize the relevance of bacterial lipopeptide production for competitive interactions with coexisting bacteria. Furthermore, the findings reported here broaden our understanding of bacteria-derived compounds that might directly influence bacterial pathogen colonization in the animal gut. The mechanism of massetolide E-mediated pathogen growth inhibition has yet to be defined.

Our results indicate that direct microbial antagonism is important for the protective effect mediated by MYb11 and MYb12 observed in the context of BT247 infection. But interestingly, Tran et al. provide evidence of a cyclic lipopeptide of the viscosin group (massetolide A) stimulating defense responses in plants, thus potentially indirectly activating the host immune response: when the roots of the tomato plant were treated with massetolide A, the leaves showed enhanced resistance to infection with the oomycete *P. infestans* [27]. As massetolide E produced by MYb11 and MYb12 seems to have no activity against Gram-negative bacteria, yet MYb11 and MYb12 also protected worms from infection by PA14, protection against PA14 infection might be mediated through indirect mechanisms. Whether

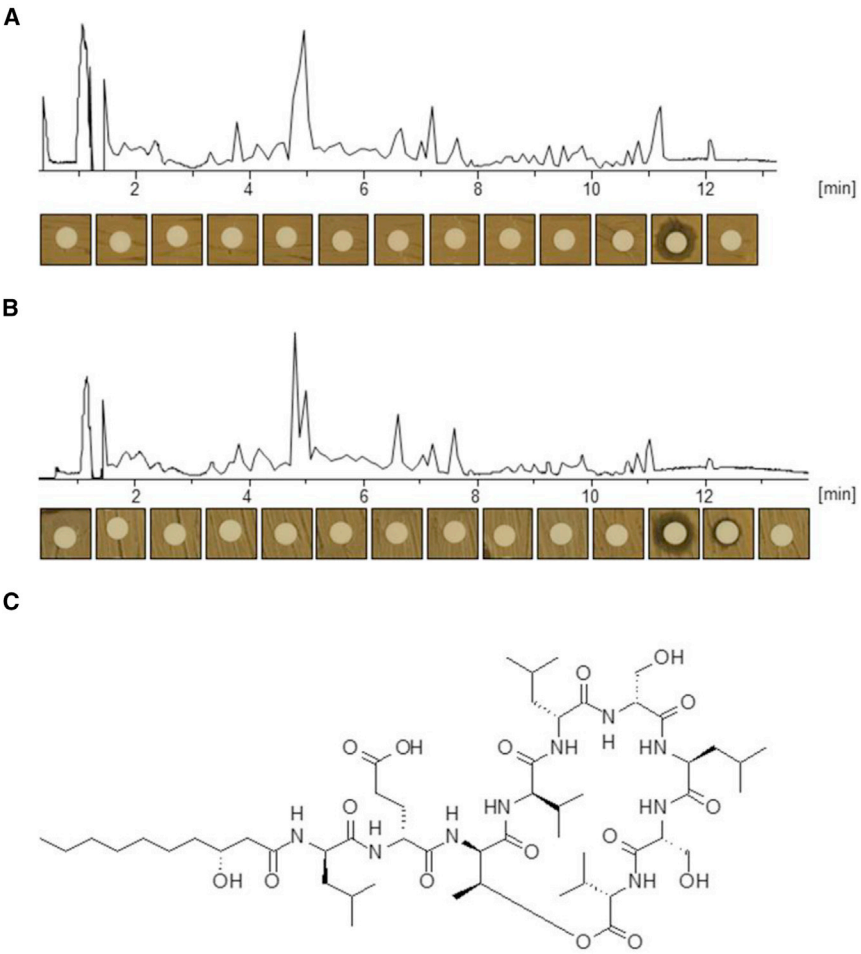

Figure 4. Identification of Massetolide E as Inhibitory Compound in Extracts from *Pseudomonas* Isolates MYb11 and MYb12

(A and B) Base peak chromatograms of extracts from (A) MYb11 and (B) MYb12 with images of the disc diffusion assay showing the bioactivity of 0.8-min fractions correlating to the respective portion of the chromatogram against *B. thuringensis* BT679 (BT247 looked identical).

(C) Structure of the antibiotic depsipeptide massetolide E. The stereochemistry of massetolide E is derived from domain organization of the NRPS and known massetolide structures.

See also Figures S3 and S4.

MYb11 and MYb12 can also protect *C. elegans* from pathogen infection through an indirect mechanism and if massetolide E contributes to this effect remains to be determined.

Conclusion

We identify a defined function for members of the native microbiota of the model nematode *C. elegans*: our work suggests that three microbiota isolates of the *P. fluorescens* species complex protect the worm against infection with the natural *C. elegans* pathogen *B. thuringiensis* through distinct mechanisms. The two isolates MYb11 and MYb12 directly inhibit pathogen growth, likely through the production of massetolide E, a cyclic lipopeptide of the viscosin group. In contrast, the isolate MYb115 limits pathogen-induced damage without inhibiting pathogen growth, likely through an indirect, host-defense-dependent mechanism. These findings provide novel insights into the function of the native microbiota of the model nematode *C. elegans*, highlighting the role of microbes in supporting the worm immune response. Moreover, the identification of massetolide E broadens our understanding of microbiota-derived compounds that might directly influence pathogen colonization in the animal gut. Thus, our study strengthens the potential of *C. elegans* as a model for the identification of immune-protective mechanisms, which is key for the development of microbiota-based therapeutic strategies.

STAR★METHODS

Detailed methods are provided in the online version of this paper and include the following:

- KEY RESOURCES TABLE
- CONTACT FOR REAGENT AND RESOURCE SHARING
- EXPERIMENTAL MODEL AND SUBJECT DETAILS
  - Nematode strains and maintenance
  - Bacterial strains and maintenance
- METHOD DETAILS
  - Population growth assay
  - Survival assay
  - Pathogen load assay
  - Disc diffusion assay
  - Intestinal barrier function assay
  - Genomic analyses
  - UPLC- high resolution mass spectrometry
  - Preparative high-performance liquid chromatography
- QUANTIFICATION AND STATISTICAL ANALYSIS
- DATA AND SOFTWARE AVAILABILITY

SUPPLEMENTAL INFORMATION

Supplemental Information can be found with this article online at https://doi.org/10.1016/j.cub.2019.01.050.

ACKNOWLEDGMENTS

We thank Hinrich Schulenburg for generous intellectual input, advice, and support; Barbara Pees and Alejandra Zárate-Potes for helpful discussions; the Schulenburg group for valuable feedback; and the Caenorhabditis Genetics Center (University of Minnesota, Minneapolis, Minnesota, USA), which is funded by NIH Office of Research Infrastructure Programs (P40 OD010440). We also thank Susanne Landis (https://www.scienstration.com/) for creating the graphical abstract. This work was funded by the German Science Foundation DFG (Collaborative Research Center CRC1182 Origin and Function of Metaorganisms, Project A1.2 to K.D. and Project INF to C.K.), Germany. Work in the Bode lab was supported by the LOEWE Center Translational Biodiversity Genomics (TBG) funded by the state of Hesse, Germany.

AUTHOR CONTRIBUTIONS

K.D. conceived the study and secured funding. K.A.B.K. and K.D. designed the experiments, analyzed the data, and wrote the manuscript. M.D. and H.B.B. did the UPLC-HRMS, HPLC, and genomic analyses. J.Z. and C.K. analyzed the genomic data. E.-L.S. and K.A.B.K. conducted the PA14 experiments. K.A.B.K. conducted all other experiments.

DECLARATION OF INTERESTS

The authors declare no competing interests.

Received: November 20, 2018
Revised: December 21, 2018
Accepted: January 18, 2019
Published: February 28, 2019

REFERENCES

1. Dirksen, P., Marsh, S.A., Braker, I., Heitland, N., Wagner, S., Nakad, R., Mader, S., Petersen, C., Kowallik, V., Rosenstiel, P., et al. (2016). The native microbiome of the nematode *Caenorhabditis elegans*: gateway to a new host-microbiome model. BMC Biol. *14*, 38.
2. Round, J.L., and Mazmanian, S.K. (2009). The gut microbiota shapes intestinal immune responses during health and disease. Nat. Rev. Immunol. *9*, 313–323.
3. Ubeda, C., Djukovic, A., and Isaac, S. (2017). Roles of the intestinal microbiota in pathogen protection. Clin. Transl. Immunology *6*, e128.
4. Geudens, N., and Martins, J.C. (2018). Cyclic lipodepsipeptides from *Pseudomonas spp*. – biological swiss-army knives. Front. Microbiol. *9*, 1867.
5. Raaijmakers, J.M., De Bruijn, I., Nybroe, O., and Ongena, M. (2010). Natural functions of lipopeptides from *Bacillus* and *Pseudomonas*: more than surfactants and antibiotics. FEMS Microbiol. Rev. *34*, 1037–1062.
6. Zhang, F., Berg, M., Dierking, K., Félix, M.A., Shapira, M., Samuel, B.S., and Schulenburg, H. (2017). *Caenorhabditis elegans* as a model for microbiome research. Front. Microbiol. *8*, 485.
7. Nelder, J.A., and Wedderburn, R.W.M. (1972). Generalized linear models. J. R. Stat. Soc. Ser. Ser. A *135*, 370–384.
8. Dunn, O.J. (1961). Multiple comparisons among means. J. Am. Stat. Assoc. *56*, 52–64.
9. Kaplan, E.L., and Meier, P. (1958). Nonparametric estimation from incomplete observations. J. Am. Stat. Assoc. *53*, 457–481.
10. Dunnett, C.W. (1955). A multiple comparison procedure for comparing several treatments with a control. J. Am. Stat. Assoc. *50*, 1096–1121.
11. Kim, D.H. (2013). Bacteria and the aging and longevity of *Caenorhabditis elegans*. Annu. Rev. Genet. *47*, 233–246.
12. Montalvo-Katz, S., Huang, H., Appel, M.D., Berg, M., and Shapira, M. (2013). Association with soil bacteria enhances p38-dependent infection resistance in *Caenorhabditis elegans*. Infect. Immun. *81*, 514–520.
13. Kim, D.H., and Ewbank, J.J. (2018). Signaling in the innate immune response. Wormbook *2018*, 1–35.
14. Tan, M.W., Rahme, L.G., Sternberg, J.A., Tompkins, R.G., and Ausubel, F.M. (1999). *Pseudomonas aeruginosa* killing of *Caenorhabditis elegans* used to identify *P. aeruginosa* virulence factors. Proc. Natl. Acad. Sci. USA *96*, 2408–2413.
15. Chiu, L., Bazin, T., Truchetet, M.-E., Schaeverbeke, T., Delhaes, L., and Pradeu, T. (2017). Protective microbiota: from localized to long-reaching co-immunity. Front. Immunol. *8*, 1678.
16. Ford, S.A., and King, K.C. (2016). Harnessing the power of defensive microbes: evolutionary implications in nature and disease control. PLoS Pathog. *12*, e1005465.
17. Hollensteiner, J., Poehlein, A., Spröer, C., Bunk, B., Sheppard, A.E., Rosenstiel, P., Schulenburg, H., and Liesegang, H. (2017). Complete genome sequence of the nematicidal *Bacillus thuringiensis* MYBT18247. J. Biotechnol. *260*, 48–52.
18. Wang, J., Nakad, R., and Schulenburg, H. (2012). Activation of the *Caenorhabditis elegans* FOXO family transcription factor DAF-16 by pathogenic *Bacillus thuringiensis*. Dev. Comp. Immunol. *37*, 193–201.
19. Gelino, S., Chang, J.T., Kumsta, C., She, X., Davis, A., Nguyen, C., Panowski, S., and Hansen, M. (2016). Correction: Intestinal Autophagy Improves Healthspan and Longevity in C. elegans During Dietary Restriction. PLoS Genet. *12*, e1006271.
20. Ripert, G., Racedo, S.M., Elie, A.-M., Jacquot, C., Bressollier, P., and Urdaci, M.C. (2016). Secreted compounds of the probiotic *Bacillus clausii* strain o/c inhibit the cytotoxic effects induced by *Clostridium difficile* and *Bacillus cereus* toxins. Antimicrob. Agents Chemother. *60*, 3445–3454.
21. Weber, T., Charusanti, P., Musiol-Kroll, E.M., Jiang, X., Tong, Y., Kim, H.U., and Lee, S.Y. (2015). Metabolic engineering of antibiotic factories: new tools for antibiotic production in actinomycetes. Trends Biotechnol. *33*, 15–26.
22. de Bruijn, I., de Kock, M.J., Yang, M., de Waard, P., van Beek, T.A., and Raaijmakers, J.M. (2007). Genome-based discovery, structure prediction and functional analysis of cyclic lipopeptide antibiotics in *Pseudomonas* species. Mol. Microbiol. *63*, 417–428.
23. Gerard, J., Lloyd, R., Barsby, T., Haden, P., Kelly, M.T., and Andersen, R.J. (1997). Massetolides A-H, antimycobacterial cyclic depsipeptides produced by two *pseudomonads* isolated from marine habitats. J. Nat. Prod. *60*, 223–229.
24. Reder-Christ, K., Schmidt, Y., Dörr, M., Sahl, H.-G., Josten, M., Raaijmakers, J.M., Gross, H., and Bendas, G. (2012). Model membrane studies for characterization of different antibiotic activities of lipopeptides from *Pseudomonas*. Biochim. Biophys. Acta *1818*, 566–573.
25. Iatsenko, I., Yim, J.J., Schroeder, F.C., and Sommer, R.J. (2014). *B. subtilis* GS67 protects *C. elegans* from Gram-positive pathogens via fengycin-mediated microbial antagonism. Curr. Biol. *24*, 2720–2727.
26. Piewngam, P., Zheng, Y., Nguyen, T.H., Dickey, S.W., Joo, H.-S., Villaruz, A.E., Glose, K.A., Fisher, E.L., Hunt, R.L., Li, B., et al. (2018). Pathogen elimination by probiotic *Bacillus* via signalling interference. Nature *562*, 532–537.
27. Tran, H., Ficke, A., Asiimwe, T., Höfte, M., and Raaijmakers, J.M. (2007). Role of the cyclic lipopeptide massetolide A in biological control of *Phytophthora* infestans and in colonization of tomato plants by *Pseudomonas fluorescens*. New Phytol. *175*, 731–742.
28. Weber, T., Blin, K., Duddela, S., Krug, D., Kim, H.U., Bruccoleri, R., Lee, S.Y., Fischbach, M.A., Müller, R., Wohlleben, W., et al. (2015). antiSMASH 3.0-a comprehensive resource for the genome mining of biosynthetic gene clusters. Nucleic Acids Res. *43* (W1), W237-43.
29. Brenner, S. (1974). The genetics of *Caenorhabditis elegans*. Genetics *77*, 71–94.
30. Borgonie, G., Van Driessche, R., Leyns, F., Arnaut, G., De Waele, D., and Coomans, A. (1995). Germination of Bacillus thuringiensis spores in

bacteriophagous nematodes (Nematoda: Rhabditida). J. Invertebr. Pathol. *65*, 61–67.

31. Nakad, R., Snoek, L.B., Yang, W., Ellendt, S., Schneider, F., Mohr, T.G., Rösingh, L., Masche, A.C., Rosenstiel, P.C., Dierking, K., et al. (2016). Contrasting invertebrate immune defense behaviors caused by a single gene, the *Caenorhabditis elegans* neuropeptide receptor gene *npr-1*. BMC Genomics *17*, 280.

32. Kirienko, N.V., Cezairliyan, B.O., Ausubel, F.M., and Powell, J.R. (2014). Pseudomonas aeruginosa PA14 pathogenesis in Caenorhabditis elegans. Methods Mol. Biol. *1149*, 653–669.

33. Tobias, N.J., Wolff, H., Djahanschiri, B., Grundmann, F., Kronenwerth, M., Shi, Y.M., Simonyi, S., Grün, P., Shapiro-Ilan, D., Pidot, S.J., et al. (2017). Natural product diversity associated with the nematode symbionts *Photorhabdus* and *Xenorhabdus*. Nat. Microbiol. *2*, 1676–1685.

STAR★METHODS

KEY RESOURCES TABLE

REAGENT or RESOURCE	SOURCE	IDENTIFIER
Bacterial and Virus Strains		
Escherichia coli (OP50)	Caenorhabditis Genetics Center	N/A
Bacillus thuringiensis MYBT18247 (BT247)	Agriculture Research Service Patent Culture Collection of Microorganisms and Cell Cultures-NRRL (United States Department of Agriculture, Peoria, Illinois, USA). Isolated initially from NRRL-BT18247.	N/A
Bacillus thuringiensis BT407	Christina Nielsen-LeRoux (INRA-France).	N/A
Bacillus thuringiensis MY18679 (BT679)	Agriculture Research Service Patent Culture Collection of Microorganisms and Cell Cultures -NRRL (United States Department of Agriculture, Peoria, Illinois, USA). Isolated initially from NRRL-BT18679.	N/A
Pseudomonas aeruginosa PA14	Jonathan Ewbank	N/A
MYb6 (*Ochrobactrum sp. BS30*)	Natural isolate from Kiel, Schleswig-Holstein, Germany [1];	N/A
MYb10 (*Acinetobacter sp.* 'LB BR 12338')	Natural isolate from Kiel, Schleswig-Holstein, Germany [1];	N/A
Myb15 (*Ochrobactrum sp.* BS30)	Natural isolate from Kiel, Schleswig-Holstein, Germany [1];	N/A
MYb49 (*Ochrobactrum sp.* LC497)	Natural isolate from Kiel, Schleswig-Holstein, Germany [1];	N/A
MYb70 (*Ochrobactrum pseudogrignonense*)	Natural isolate from Kiel, Schleswig-Holstein, Germany [1];	N/A
MYb237 (*Ochrobactrum sp.)*	Natural isolate from Kiel, Schleswig-Holstein, Germany; this paper.	N/A
MYb71 (*Ochrobactrum sp*. R-26465)	Natural isolate from Kiel, Schleswig-Holstein, Germany [1];	N/A
MYb11 (*Pseudomonas lurida*)	Natural isolate from Kiel, Schleswig-Holstein, Germany; this paper.	N/A
MYb12 (*Pseudomonas lurida*)	Natural isolate from Kiel, Schleswig-Holstein, Germany; this paper.	N/A
MYb115 (*Pseudomonas fluorescens*)	Natural isolate from Kiel, Schleswig-Holstein, Germany; this paper.	N/A
MYb185 (*Pseudomonas denitrificans*)	Natural isolate from Kiel, Schleswig-Holstein, Germany; this paper	N/A
MYb187 (*Pseudomonas alkylphenolia)*	Natural isolate from Kiel, Schleswig-Holstein, Germany; this paper	N/A
MYb193 (*Pseudomonas lurida*)	Natural isolate from Kiel, Schleswig-Holstein, Germany; this paper	N/A
Staphylococcus aureus (SA113)	Andreas Peschel	N/A
MYb258 (*Leukobacter tardus*)	Natural isolate from Kiel. Isolated by Julia Johnke; this paper.	N/A
MYb53 (*Rodococcus erythropolis*)	Natural isolate from Kiel, Schleswig-Holstein, Germany [1];	N/A
Serratia marcescens (Db11)	Jonathan Ewbank	N/A
Pseudomonas fluorescens	Hinrich Schulenburg	N/A
Photorhabdus luminescens (Jm12)	Hinrich Schulenburg	N/A
Pseudomonas aeruginosa (PA01)	Wolfgang Streit	N/A
Chemicals, Peptides, and Recombinant Proteins		
Tetramisole hydrochloride	Sigma-Aldrich	Lot#SLBN8309V
Triton X-100	Biochemica	Lot#8W002155
Erioglaucine disodium salt	Sigma-Aldrich	Lot#MKBX7318
Zirconia beads (1mm diameter)	BioSpec Products	Cat#11079110
Sodium azide	Roth	Art#K305.1

(*Continued on next page*)

Continued

REAGENT or RESOURCE	SOURCE	IDENTIFIER
Deposited Data		
MYb11 genome sequence	NCBI	GenBank: BioSample SAMN07581396
MYb12 genome sequence	NCBI	GenBank: BioSample SAMN07581345
Experimental Models: Organisms/Strains		
C. elegans: Strain wild-type N2	Caenorhabditis Genetics Center	WB Strain: N2
C. elegans: Natural isolate MY316	Natural isolate from Kiel, Schleswig-Holstein, Germany [1];	N/A
Software and Algorithms		
RStudio	GNU	Version1.0.153
ggplot: Various R Programming Tools for Plotting Data.	R package	Version 1.0.153
SPSS	IBM®SPSS®STATISTICS	Version 24.0
Inkscape	GNU	Version 0.92
ImageJ	NIH image	RRID: SCR_003070
Image Lab	Biorad Laboratories	Version 5.2.1
AntiSMASH	[28]	Version 3.0
Other		
Ampicillin Natriumsalz	Roth	Art#K029.1
Gentamycin sulfat-Lösung	Roth	Art#HN09.2

CONTACT FOR REAGENT AND RESOURCE SHARING

Further information and requests for resources and reagents should be directed to and will be fulfilled by the Lead Contact, Katja Dierking (kdierking@zoologie.uni-kiel.de).

EXPERIMENTAL MODEL AND SUBJECT DETAILS

Nematode strains and maintenance

Maintenance of C. elegans *strains*

Caenorhabditis elegans N2 strain and *C. elegans* MY316 strain were grown and maintained on nematode growth media (NGM) seeded with the *Escherichia coli* strain OP50 at 20°C. The NGM-OP50 lawn was prepared by streaking *E. coli* OP50 from a frozen stock onto Tryptic Soy Agar (TSA) plates, followed by an overnight incubation at 37°C. A single fresh colony was then picked, inoculated in Tryptic Soy Broth (TSB), and grown overnight in a shaker-incubator at 37°C. 500 μl of the culture was seeded on NGM plates and stored at 20°C until use [29].

Synchronization of C. elegans *populations*

Worm populations were synchronized by bleaching prior to each experiment: Worms were grown on NGM-OP50 plates. Plates with gravid hermaphrodites and eggs were washed with M9 buffer, and bleached using alkaline hypochlorite solution (1ml of 5M NaOH and 1ml of NaClO 12% bleach), followed by multiple washes with M9 buffer. L1s were allowed to hatch in M9 buffer overnight at 20°C. Next, L1 larvae were transferred to fresh NGM-OP50 plates, and incubated at 20°C. Fourth instar larval (L4) stage hermaphrodite nematodes were used in all infection assays (described in detail below). One day adult hermaphrodite nematodes were used for the intestinal barrier function assay (described in detail below).

Bacterial strains and maintenance

C. elegans *microbiota isolates and* E. coli *OP50*

Natural *C. elegans* microbiota isolates from Northern Germany, originating from the *C. elegans* wild isolate MY316 or its substrate, were used [1]. The natural microbiota isolates and the *E. coli* OP50 control were grown on TSA plates at 25°C and cultured in TSB in a shaker-incubator overnight at 28°C.

Bacillus thuringiensis strains

Spore-enriched cultures of *Bacillus thuringiensis* strains (MYBT247, MYBT679, and MYBT407) were obtained following a protocol established by Borgonie et al. [30] with some modifications as described in detail in the following: *B. thuringiensis* (BT) strains were thawed from frozen stocks and streaked onto Luria-Bertani (LB) plates, followed by an overnight incubation at 25°C. A sterile pipette tip was used to scrape off bacteria from the plate and ejected into LB medium for an overnight incubation at 28°C. 1 mL of overnight *B. thuringiensis* culture was then transferred into 1000 mL of sterile BT medium (Bacto-peptone (Sigma) (7.5 g/l), glucose

(5.56 mM), KH_2PO_4 (22.06 mM), K_2HPO_4 (22.99 mM), pH adjusted to 7.2) with 5 mL of filter-sterilized salt solution ($MgSO_4.7H_2O$ (100 mM), $MnSO_4$.H2O (2.37 mM), $ZnSO_4.7H_2O$ (9.76 mM), $FeSO_4.7H_2O$ (14.39 mM)) and 1250 μl of $CaCl_2$ (1M). Cultures were incubated in a shaker-incubator at 120 rpm and 28°C for seven days. On day 4 of incubation 5 mL of salt solution and 1250 μl of 1M $CaCl_2$ was again added to the culture medium.The spore-crystal solution was harvested by centrifugation of the culture in 50 mL Falcon tubes (SARSTEDT) at 3000 rpm for 10 min. The pelleted particles were resuspended in Phosphate Buffered Saline (PBS), and the number of particles were counted using the Neubauer counting chamber method. The aliquots were stored in 1 mL tubes, at −20°C, with a concentration range of 10^9-10^{10} particles/mL for BT247 and BT679, and a concentration range of 10^3-10^4 particles/mL for BT407. BT spore solution aliquots were freshly thawed before every infection experiment.

Pseudomonas aeruginosa PA14

The *Pseudomonas aeruginosa* PA14 strain was grown on LB Agar (LBA) plates and cultured overnight at 37°C in LB broth prior to the infection assay, which is described in detail below.

METHOD DETAILS

Population growth assay

The population growth assay was used as a proxy to measure worm fitness by extrapolating the offspring produced by a single worm after two generations. Peptone-free medium (PFM) plates were used in all assays with BT to avoid the germination of spores on plates. PFM plates were seeded with a 500 μl-lawn a BT spore solution of BT407, BT247 or BT679 mixed with an overnight culture of each of the tested microbiota isolate, adjusted to an OD_{600} of 10 with PBS. The concentration of the BT-microbiota mixes were 1:50 for the non-pathogenic control BT407 and a concentration of 1:200 for BT247 and BT679. The lawns were allowed to dry overnight at a temperature of 20°C. Three worms at the L4 stage were picked using a platinum wire onto the respective lawns, and incubated at 20°C for 5 days. The produced worm populations were then washed off the plates using 2 mL M9T (M9 buffer and 0.1% Triton) and frozen in 2 mL tubes at −20°C until counting of worms. The tubes were thawed and weighed prior to counting of worms, to correct for volumes lost during the washing procedure. From each tube a 10 μl aliquot was used to count the number of worms, and the average of three independent aliquot counts from each sample was used to extrapolate the offspring produced from an individual worm. A control treatment group with OP50 mixed with each of the three BT strains was included in every run. The population growth assay was repeated for at least three independent runs with each of the two worm strains N2 and MY316. All treatments were randomized by initiating random codes on plates, to prevent experimenter bias.

The protective effect of the microbiota isolates on the population growth was analyzed in triplicates using a linear model framework (GLM), where the population growth of the worms after 5 days was incorporated as the dependent variable and the microbiota isolates and the pathogen strains as fixed factors independently. The post hoc analysis was done using the Tukey test and Bonferroni based adjustment was used to correct for multiple comparison testing [8].

Survival assay

Bacillus thuringiensis survival assay

B. thuringiensis survival assays were done according to a standardized protocol [31]. Accordingly, 6 cm PFM plates were inoculated with 75μl of each of the microbiota isolates or OP50, adjusted to OD_{600} of 10, mixed with different dilutions (1:5, 1:10, 1:25, 1:50) of the BT247 spore solution. For the non-pathogenic BT407 control the highest dilution (1:5) was used, mixed with each of the microbiota isolates or OP50. The plates were left to dry overnight at 20°C. On the infection day, 30 L4 nematodes were placed on each of the previously randomized plates, followed by incubation at 20°C. Worms were assessed as alive or dead using gentle touching with a sterile platinum wire. Alive and dead worms were counted 24h post-infection. Escaped worms were censored. For experiments with heat-inactivated bacteria, overnight cultures of the bacteria, prepared as described above, were adjusted to an OD_{600} of 10, and afterward were heat-inactivated by incubation at 80°C for a duration of 2h.

All BT survival assays were done in at least three independent runs with four technical replicates per treatment group in each run.

We used GLM analysis to evaluate the effects of the microbiota isolates on the survival of worms when challenged with each of the BTs across the concentration range of each of the different BT strains, using worm survival as dependent variable and each of the microbiota isolates and the BT concentration as fixed factors. The post hoc analysis was done using the Tukey test and corrections for multiple comparison testing with the OP50 control treatment group were done by Bonferroni based adjustment.

Pseudomonas aeruginosa survival assay

P. aeruginosa PA14 survival assay were done following the protocol described in Kirienko et al. [32] with minor modifications, as described in the following: Worms were bleached and maintained on the respective microbiota or OP50 lawn from the L1 stage until the L4 stage, as described above. Then worms were washed off with M9 and 30 worms were transferred to each slow killing infection (SK) plate that were inoculated with 10 μl of overnight culture of either PA14 or OP50, followed by a 24 h incubation at 37°C and another 24 h incubation at 25°C. SK plates are enriched NGM plates (containing 0.35% instead of 0.25% peptone), which ensure efficient ''slow killing'' of worms [14].

Alive and dead worms were scored every 24 h, while the surviving worms were transferred to new SK plates. Survival assays were performed in at least three independent runs with four technical replicates per treatment group in each run. The data of the runs were pooled and analyzed by Kaplan-Meier and log rank test, and corrected for multiple testing with Bonferroni, using the platform RStudio (Version1.0.153).

Pathogen load assay

Pathogen load assay was done by counting BT247 colony forming units (CFUs) as follows: Worms were grown on NGM-OP50 plates until the L4 stage and then exposed to each of the microbiota isolates or *E. coli* OP50 at an OD_{600} of 10 mixed with BT247 spores at a concentration of 1:25. 24h post-infection ten adult worms were placed into tubes containing M9 buffer and 25 mM Tetramisole (TM buffer) using a hair picker. The supernatant was removed and the worms were washed twice with TMG buffer containing gentamicin (100 μg/mL) in TM buffer, and twice with M9 buffer. The last M9 washing buffer was transferred to another tube to serve as a washing control. Finally, 100 μL of PBST (PBS with 1% Triton X-100) was added to the tubes containing the worms. Sterile zirconia beads (1 mm in diameter) were then added to the tubes containing both the worms and the control supernatant and the samples were homogenized using the GenoGrinder200. The resulting suspension was serially diluted (10^{-1}-10^{-6}) with PBS and plated on TSA plates, for the subsequent growing and counting of BT colonies, after an incubation at 25°C for 24-48h.

The CFU score of the washing control was subtracted from the CFU score of the worm samples and divided by the number of worms recorded in the last washing step. The experiment was done in three independent runs with six technical replicates each. Students pairwise t test followed by Bonferroni correction for multiple testing was performed [8]. Results were considered significant when P-value ≤ 0.05. All treatments were randomized initiating random codes on plates and tubes, to prevent experimenter bias.

Disc diffusion assay

Kirby-Bauer disk diffusion method was performed in accordance with the guidelines of the Clinical and Laboratory Standards Institute (CLSI) and with the following modifications. Microbiota isolates, *E. coli* OP50 and BT247 or PA14 were grown in TSB in a shaker incubator overnight at 28°C. The bacterial suspensions were adjusted to an OD_{600} of 10 with PBS. Culture supernatants were filtered with a 0.2-micron filter (SARSTEDT) to obtain cell-free supernatants. Mueller Hinton agar plates (9 cm in diameter) having a depth of 4mm of the medium were inoculated with each of the three BTs or PA14, using a cotton swab to evenly distribute the inoculums on the plate. Sterile Whatman (6mm in diameter) discs (GE healthcare) were inoculated with 15μl of the microbiota isolates' or *E. coli* OP50 filtered supernatant and placed on each of the BT or PA14 inoculated plates. 15 μl ampicillin (50 mg/mL) was used as positive control for BT and 15 μl gentamicin (20 mg/mL) was used as positive control for PA14. The plates were incubated for 48 h at 25°C. Images of each plate were taken using the ChemiDocTouch Imaging system (GelDoc Camera, BioRAD) and analyzed with subsequent Image lab software (Version 5.2.1). Zones of inhibition were measured with ImageJ (1.50e, NIH, USA). The assays were performed in at least three independent runs for each pathogen, with three technical replicates for each treatment group in each run.

The effects of MYb11 and MYb12 non-filtered supernatants on growth of six Gram-positive and 5 Gram-negative bacteria (Figure S2) was tested as described above. The bacterial suspensions were adjusted to an OD_{600} of 1 with PBS. TSB was used as negative control.

Student's t test was used to evaluate the differences in means of the diameter of the zones of inhibition produced in the three runs (each run having three technical replicates), in comparison to the control OP50 treatment group. A Bonferroni based adjustment was used to correct for multiple comparison testing with the control. All treatments were randomized initiating random codes on plates, to prevent experimenter bias.

Intestinal barrier function assay

Nematodes were raised and infected as described in the pathogen load assay above and treated according to a published protocol by Gelino et al. [19] as described in detail in the following: Worms were washed off the infection plates with 5 mL S buffer (NaCl (100 mM), K_2HPO_4 (6.5 mM), and KH_2PO_4 (43.5 mM)) 24 h post-infection and suspended in a liquid suspension (1:1) of S buffer mixed with blue food dye (Erioglaucine disodium salt, Sigma-Aldrich, 5.0% wt/vol in water) for 3 h.

Animals were then washed three times with S buffer, centrifuged at 3500 rpm for 1 min, and 20 μl of the pellet was mounted on microscopic slides padded with 2% Agarose. 10 μl Sodium azide (20 mM) was added to paralyze the worms. The worms were visually analyzed for the presence and/or the absence of leaked blue dye outside the intestinal lumen and throughout the body cavity using a Leica dissecting microscope (LEICA M205 FA). The percentage of "smurf" worms was calculated per treatment, each plate containing at least 30 worms. The assay was performed in two independent runs with four technical replicates each. Student's pairwise t test and Bonferroni based adjustment was used to correct for multiple testing with the OP50 control treatment group. All treatment groups were randomized to avoid observer bias.

Genomic analyses

MYb11 and MYb12 sequences are available from NCBI GenBank, Bioproject PRJNA400855. antiSMASH [28] was used to search for known biosynthetic gene clusters (BGCs) in both genomes.

UPLC- high resolution mass spectrometry

The Ultra performance liquid chromatography high resolution mass spectrometry (UPLC-HRMS) analyses were performed with an UltiMate 3000 system (Thermo Fisher) coupled to an Impact II qToF mass spectrometer (Bruker) as described previously [33]. ACN with 0.1% formic acid in H_2O was used as solvent. The flow rate was set at 0.4 mL min^{-1} with a gradient from 5% ACN to 95% ACN over 15 min. The mass spectrometer was calibrated using 10 mM sodium formate before data acquisition. The MS method used for data acquisition also included an internal calibrant window before the data acquisition of each biological sample where 10 mM sodium formate were injected. The internal calibrant was used by Bruker DataAnalysis to correct the acquired mass data. The following

MS settings were used for data acquisition: source settings: capillary voltage 4500 V, nebulizer nitrogen gas pressure 3 bar, ion source temperature 200°C, dry gas flow 8 L min^{-1}; scan settings: ion polarity positive, mass range 90 to 1500, spectra rate 3 Hz; tune parameters: transfer funnel 1 RF 300 Vpp, funnel 2 RF 300 Vpp, isCID off, hexapole RF 60 Vpp; stepping settings: (i) 0 ms, collision RF 500, transfer time 82.5 μs, collision energy 65%; (ii) 25 ms, collision RF 500, transfer time 82.5 μs, collision energy 85%; (iii) 45 ms, collision RF 500, transfer time 82.5 μs, collision energy 100%; (iv) 75 ms, collision RF 500, transfer time 82.5 μs, collision energy 130%; MS/MS settings: 8 precursor ions, threshold 1000 counts (absolute), activated active exclusion after 3 spectra and 0.5 min release time, active precursor reconsidering factor 4, smart exclusion 2 times.

Preparative high-performance liquid chromatography

Methanolic XAD-16 extracts from 1 L cultures of MYb11 and MYb12 in M9 medium were used for fractionation. Preparative high-performance liquid chromatography (HPLC) was performed using an Agilent LC 1260 Infinity II Preparative LC/MSD System with an Agilent prep C18 column (10 μm, 30 × 250 mm) with a flow of 40 mL/min and a gradient from 5% to 100% ACN in 18 min. The ACN concentration remained at 100% for 3 min (MYb11) or 5,5 min (MYb12), respectively. 13 and 14 0.8 min-fractions were collected over time from 1,5 min to the end of the respective run. The fractions were dried and stored at −20°C. 50 μg of each fraction were used in disc diffusion assays as described above.

QUANTIFICATION AND STATISTICAL ANALYSIS

Statistical analyses were done using RStudio (Version1.0.153) and SPSS Statistics (Version 24.0). Inkscape was used for the graphical illustrations. When applicable normality of the data was examined using quantile plots and the Shapiro–Wilk normality test. Levene's test was used to inquire about the homogeneity of the variance, and proceed with the appropriate test accordingly. All pairwise comparisons were followed with Bonferroni correction for multiple testing. The detailed statistical tests used for each experiment are mentioned in the figure legends and in the method details section above, and included in the supplementary file. Significance was determined when the P-value ≤ 0.05. To avoid experimenter bias, we initiated random number codes for the treatments, incubated samples in a spatially randomized manner and evaluated the samples in a randomized order to minimize the influence of random environmental effects and observer bias.

DATA AND SOFTWARE AVAILABILITY

All analyses were performed with SPSS Statistics (Version 24.0) or RStudio (Version1.0.153) as indicated in the specific experiment sections. Graphs were plotted using the ggplot function in R, and edited in Inkscape (Version 0.92). All raw data and statistical analyses are available on Mendeley: https://data.mendeley.com/datasets/3464534ccd/draft?a=482aa37c-2ebd-4990-9b14-69383fafea3a. All custom R scripts for analyses are available upon request.

Current Biology, Volume *29*

Supplemental Information

Natural *C. elegans* Microbiota Protects against Infection via Production of a Cyclic Lipopeptide of the Viscosin Group

Kohar A.B. Kissoyan, Moritz Drechsler, Eva-Lena Stange, Johannes Zimmermann, Christoph Kaleta, Helge B. Bode, and Katja Dierking

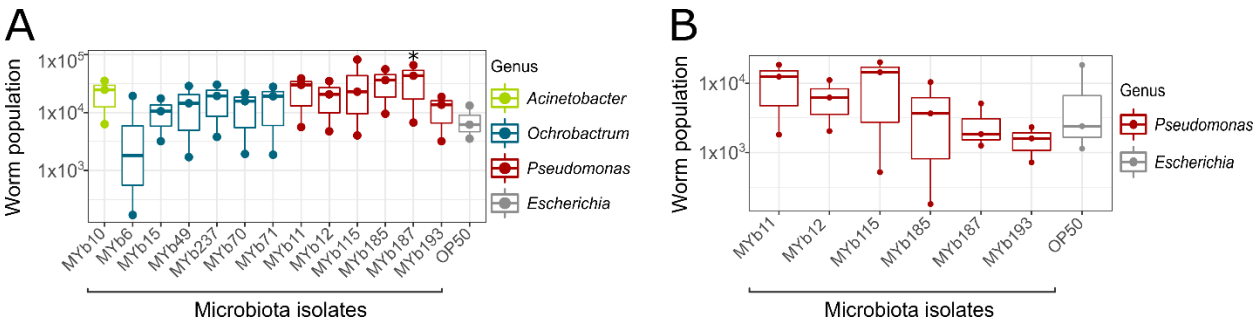

Figure S1. Natural microbiota isolates of the genus *Pseudomonas* increase *C. elegans* fitness in the presence of the non-pathogenic *B. thuringiensis* strain BT407. Related to Figure 1.

(A, B) Population size measured in the presence of non-pathogenic *B. thuringiensis* (BT407) of **(A)** the natural *C. elegans* isolate MY316 on one of 13 microbiota isolates and **(B)** the *C. elegans* N2 strain on one of 6 *Pseudomonas* isolates. *E. coli* OP50 was used as control. Three L4 larvae were picked onto the infection plates. Population size was assessed after 5 days at 20°C. The boxplots indicate the median, range and upper and lower quartiles of the worm population data (n = 3 independent runs). Statistical analysis were performed using GLM [S1] model framework and the obtained *P* values were corrected using Bonferroni correction for multiple testing [S2]. *P* values are considered significant and denoted with asterisks according to: *$P \leq 0.05$, **$P \leq 0.01$, ***$P \leq 0.001$.

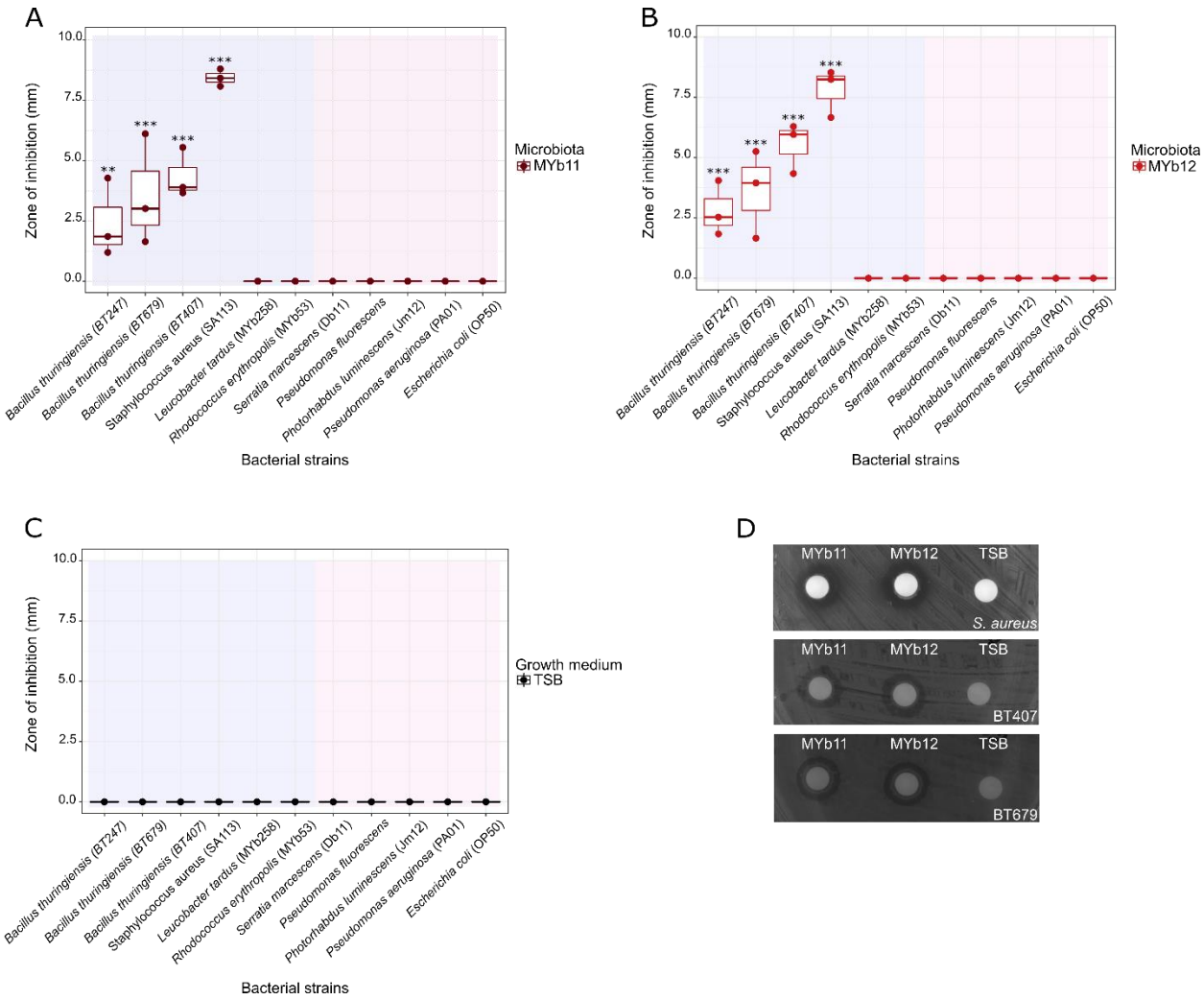

Figure S2. *Pseudomonas lurida* MYb11 and MYb12 have antagonistic activity and inhibit growth of the Gram-positive bacterial strains BT407, BT679, and *S. aureus* SA113. Related to Figure 2.

Growth inhibition of different Gram-positive and Gram-negative bacteria by supernatant of **(A)** MYb11, **(B)** MYb12, and **(C)** the TSB growth medium control, measured as diameter of inhibition zone (mm) in a disc diffusion assay. The data points represent the mean diameter of three technical replicates of three independent runs (n=3). The boxplots indicate the median, range and upper and lower quartiles of the data. The diameters are standardized by subtracting the 6 mm diameter of the disc from the overall diameter measured. Student's pairwise t-test was performed against the TSB, followed by Bonferroni correction for multiple testing. Purple shade denotes Gram-positive bacteria and pink shade denotes Gram-negative bacteria. **(D)** Representative images of the disc diffusion assay showing that supernatant of MYb11 and MYb12 inhibit growth of *S. aureus*, BT407, and BT679. *P* values are considered significant and denoted with asterisks according to: **P*≤0.05, ***P*≤0.01, ****P*≤0.001.

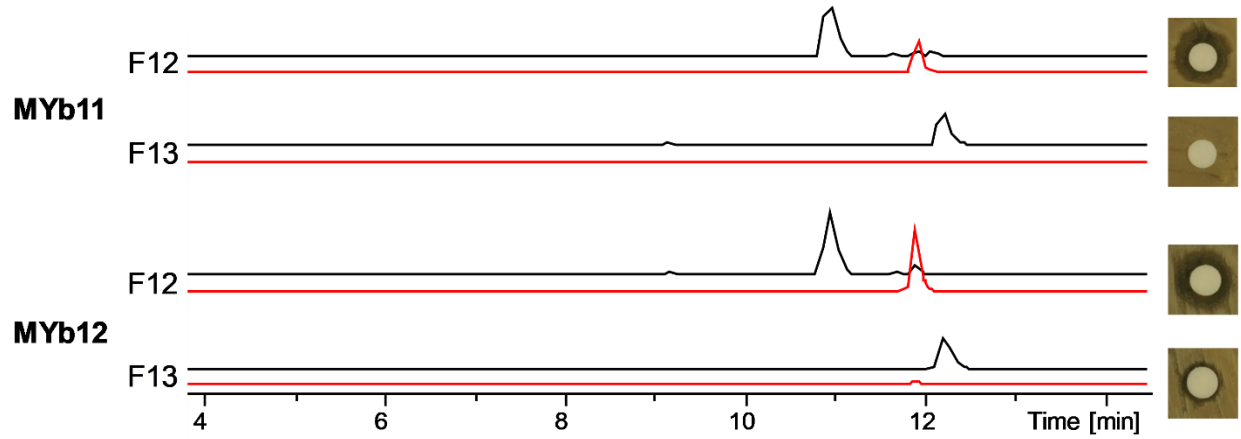

Figure S3. Base peak chromatograms (BPCs, black) and extracted ion chromatograms (EICs, red) (*m/z* 1112.66) and bioactivity of fractions 12 and 13 from *Pseudomonas* isolates MYb11 and MYb12. Related to Figure 4. Normalized BPCs and normalized EICs of fractions 12 and 13 of MYb11 and MYb12 extracts are shown. Images of the disc diffusion assay showing the bioactivity of the respective fraction against *B. thuringiensis* BT679 (BT247 looked identical) are shown next to the BPCs and EICs.

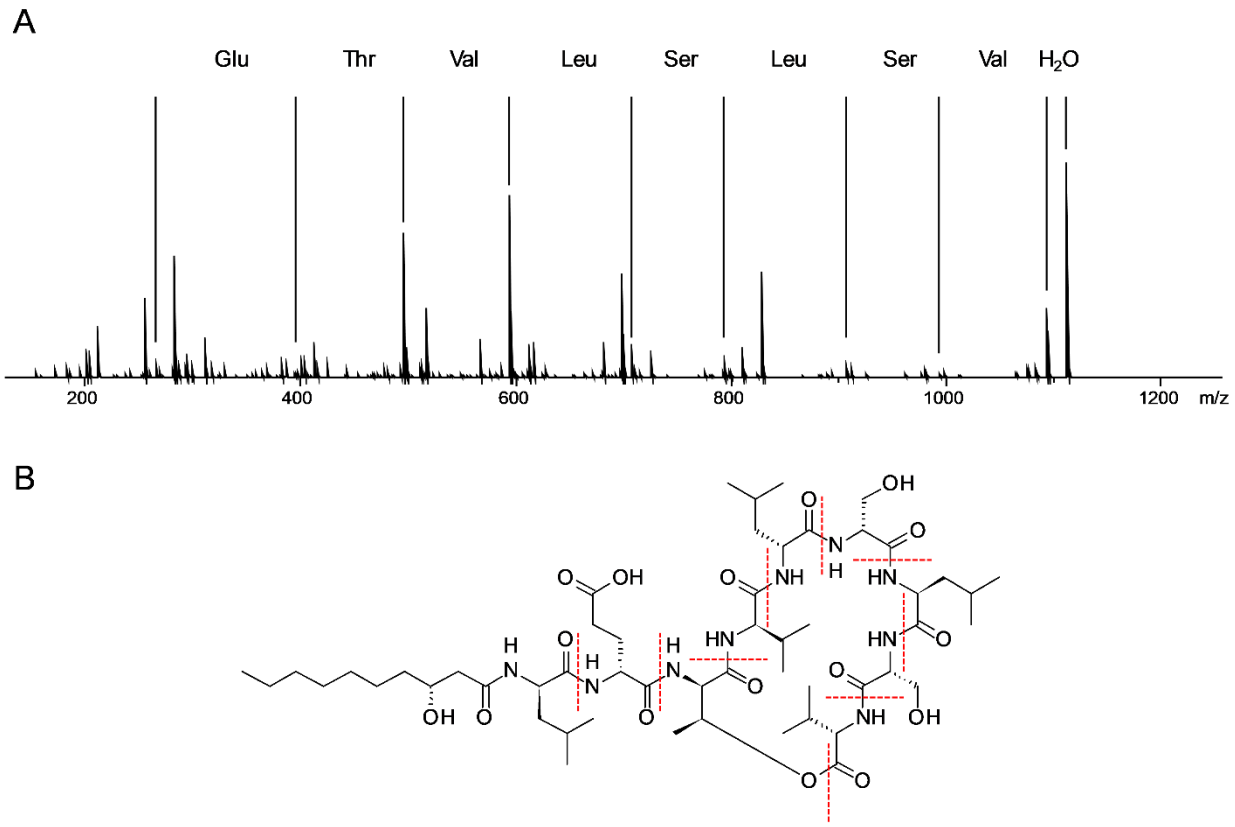

Figure S4. MS/MS fragmentation (A) and structure of massetolide E with assigned fragmentation events (B) represented by red dotted lines. Related to Figure 4.

References

[S1] Nelder, J.A., and Wedderburn, R.W.M. (1972). Generalized linear models. J. R. Stat. Soc. Ser. Gen. *135*, 370.

[S2] Dunn, O.J. (1961). Multiple comparisons among means. J. Am. Stat. Assoc. *56,* 52–64.